Int. J. Plasma Environ. Sci. Technol. 14 (2020) e02001 (9pp)

International Journal of Plasma Environmental Science and Technology

Regular Paper

DOI: 10.34343/ijpest.2020.14.e02001

Effect of ozone generation on decomposition of acetic acid by plasma in underwater bubbles

Taichi Watanabe[1, *], Shungo Zen[1], Nozomi Takeuchi[1, 2], Hyun-Ha Kim[2]

[1] Department of Electrical and Electronic Engineering, Tokyo Institute of Technology, Japan
[2] National Institute of Advanced Industrial Science and Technology (AIST), Tsukuba, Japan

* Corresponding author: watanabe@hv.ee.e.titech.ac.jp (Taichi Watanabe)

Received: 26 March 2020
Revised: 25 May 2020
Accepted: 3 June 2020
Published online: 5 June 2020

Abstract

Acetic acid is the bulk of an acid mass in so-called produced water which is generated during oil and gas extraction as a by-product. We conducted acetic acid decomposition using our plasma-based advanced oxidation process under several conditions of voltage and solution. The plasma in oxygen bubbles, with an input power of 40 W, achieved a 93% reduction of the total organic carbon (TOC) concentration after 3 h. Experiments under conditions of higher input power, lower pH, or with the use of Ar gas bubbles exhibited slower acetic acid decomposition. We concluded that the efficiency of utilization of the ozone generated by the plasma was greatly affected by the input power and pH of the solution.

Keywords: Acetic acid, advanced oxidation process (AOP), discharge plasma, ozone, solution pH, underwater bubbles.

1. Introduction

Produced water is a by-product produced during the extraction of oil and natural gas, and it contains organic matters represented by acetic acid [1]. In offshore oil plants, oil and solid matter are removed from produced water, but the treated water still contains soluble organic matters, which is becoming a serious problem as restrictions on the emission of organic compounds to the environment are becoming more stringent [2, 3]. In particular, the restriction of the quantity of organic compounds in water has become rigorous, and the need for the removal of these organic compounds in produced water has increased. One of the methods for the removal of organic compounds in produced water is the advanced oxidation process (AOP). The AOP refers to a water treatment process that uses hydroxyl radicals (OH) and has a variety of methods including the H_2O_2/O_3 method [4–7], the H_2O_2/UV method [5, 6], the UV/O_2 method [5, 6], and the O_3/catalyst method [8]. The AOP using plasma generated in contact with water has been studied for several decades. Since a plasma-based AOP directly generates hydroxyl radicals from water molecules in a treated solution, it solves problems such as the transportation and storage of high-density hydrogen peroxide, and it is one of the more promising alternatives, particularly for offshore oil plants.

Different decomposition methods with a wide range of processing speeds and efficiencies have been proposed as a plasma-based AOP for the reduction of the total organic carbon (TOC). They have shown that the hydroxyl radicals cause self-quenching right after their generation to degenerate into hydrogen peroxide which plays the role of a scavenger of hydroxyl radicals and impairs the decomposition processing speed and efficiency. To deal with the problem caused by hydrogen peroxide, we proposed an ozone–plasma system, in which ozone is added to the solution during the plasma treatment and is utilized to regenerate hydroxyl radicals through the reactions of ozone and hydrogen peroxide. The processing speed and efficiency of the decomposition of high-density acetic acid greatly improved due to the ozone addition. However, this system requires another reactor and power supply to generate ozone, which increases the capital expenditure.

To overcome this drawback, we proposed a system in which hydrogen peroxide and ozone are simultaneously generated by the same plasma reactor. It is well known that plasma in contact with water generates both [9–11]. Lukes *et al*. investigated the generation characteristic of hydrogen peroxide and ozone in different reactors. They observed a lower concentration of ozone by an order of magnitude in a reactor with

a larger current in the gas phase and they concluded that it was due to the higher gas temperature, the higher electron density, and the higher density of water vapor at the gas-liquid interface [12]. Magureanu *et al.* performed degradations of organic pollutants and pharmaceuticals using a pulsed corona discharge in contact with liquid [13–15]. They observed faster and more efficient degradation of the target materials when a plasma reactor was combined with gas bubbling. They confirmed the positive effects of the additional generation of hydroxyl radicals by reactions between ozone and hydrogen peroxide. Shimizu *et al.* measured the production of hydrogen peroxide and ozone in the liquid phase by discharges on the water surface and proved their transportation mechanism from the gas phase to the liquid phase [16]. Kuroki *et al.* decomposed phenol by discharges at the gas-liquid interface combining bubbling of hydrogen peroxide and ozone. They found that phenol was decomposed at more than twice the decomposition speed with only air and they concluded that it was because there were more hydroxyl radicals produced in the reaction of hydrogen peroxide with ozone and UV [17]. These results showed that hydroxyl radicals were generated through the reaction between ozone produced by the plasma and hydrogen peroxide. Our proposed system utilizes this reaction.

In this study, we conduct the decomposition of acetic acid by plasma in underwater bubbles under different conditions of input power, gas supply, and solution pH. The target material, acetic acid, which is the bulk of an acid mass in produced water and is one of persistent organic matter, is decomposed by hydroxyl radicals thanks to its high oxidation potential (2.8 V), which is higher than ozone. Decomposition of acetic acid in a plasma-based AOP with gas bubbles was investigated with an emphasis given to the collective analysis of ozone formation and its effective contribution to the removal of acetic acid.

2. Experimental

2.1 Experimental setup

Fig. 1 shows the experimental setup for the decomposition of acetic acid. An acrylic cylinder containing a 1 L solution, has a 1 mm thick ceramic plate at the bottom of the cylinder, with 21 individual holes (diameter 0.3 mm, adjacent distance 10 mm). Oxygen or argon gas was regulated at 2 L min^{-1} by a mass flow controller (Kofloc CR400) and streamed into the reactor from the bottom to generate gas bubbles through the 21 holes of the ceramic plate. Pin-type electrodes, connected to high-voltage, were placed 0.5 mm below the ceramic plate. Discharges were generated in the bubbles by applying an alternating high voltage to the electrodes.

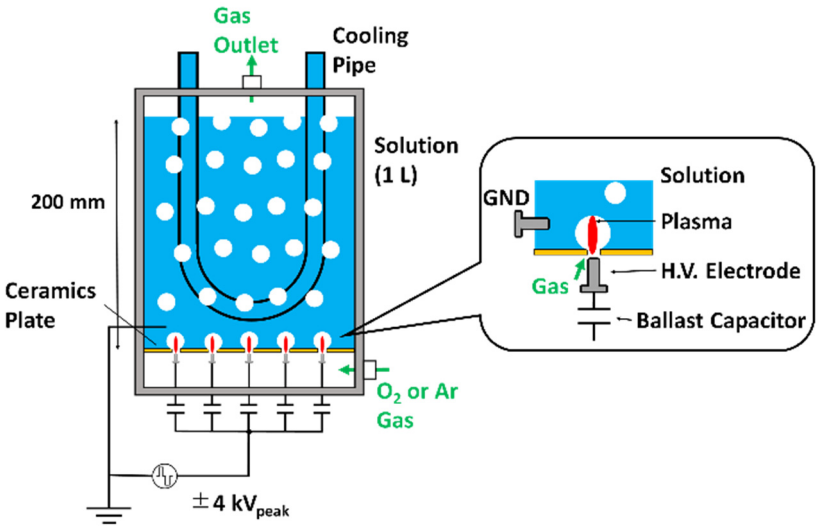

Fig.1. Experimental setup for acetic acid decomposition

The alternating applied voltage with its applying time of 25 μs was generated using a DC voltage source (PWR400M), an inverter, and a step-up transformer and it was applied to the electrodes through ballast capacitors of 15 pF or 100 pF, respectively. The applied voltage *v* and the current *i* were measured using a high voltage probe (Tektronix, P6015A) and a current transformer (Pearson Electronics, Model 2877) and they were

monitored and sampled using an oscilloscope (RIGOL, DS1104). Based on the waveform data obtained from the oscilloscope, the input power was calculated as follows,

$$P = f \int_0^T vi \, dt \quad (1)$$

where T is the period of the applied voltage.

2.2 Experimental method

Acetic acid solutions were prepared to be TOC concentration of 30 mgC L^{-1} with different pH values. One was prepared at a pH of 7.3 and a conductivity of 1.5 mS cm^{-1} by dissolving 115 mL of 0.1 mol L^{-1} phosphate buffer to reproduce the representative parameters of produced water. For the other, the pH was 4.4 without the phosphate buffer and the conductivity was set at 1.5 mS cm^{-1} by dissolving 1 g of Na_2SO_4. The solution temperature was kept at approximately 20 ℃ using a cooling pipe. Seven conditions, listed in Table 1, were compared. The discharge conditions for the decomposition by plasma in argon bubbles greatly differed from those with oxygen gas for the purpose of making the input power comparable to those for cases with oxygen gas. Since discharge is easily caused with much lower voltage application in argon atmosphere, the input power could be smaller even by an order of magnitude than those with oxygen gas. The applied voltage was chosen as the maximum voltage to sustain plasma stably and the frequency was chosen as the maximum frequency while keeping the applying time at 25 μs. During a 3-hour treatment under each condition, we sampled the solution every 30 min and measured the TOC concentrations using a TOC meter (Shimadzu, TOC-LCSN).

Fig.3. Schematic diagram of plasma reactor for GO reduction.

Table 1. Experimental conditions.

	Gas	Voltage [kV]	Frequency [kHz]	Ballast capacitor	pH	Power [W]
A	O_2	4	8	15 pF × 21	7.3	40
B	O_2	4	8	15 pF × 21	4.3	40
C	O_2	4	3	100 pF × 21	7.3	80
D	O_2	4	3	100 pF × 21	4.3	80
E	Ar	0.72	20	100 pF × 21	7.3	28
F	Ar	0.72	20	100 pF × 21	4.3	28
G	Ar	0.9	20	100 pF × 21	7.3	51

3. Results and discussion

3.1 Decomposition of acetic acid by plasma in oxygen bubbles

Fig. 2 shows the representative voltage and current waveforms during plasma generation in oxygen bubbles. Each case shows a similar waveform to the one of a dielectric-barrier discharge, which caused four-time discharges in one cycle. The peak of the current and the discharge duration increased in the case with ballast capacitors of 100 pF. This corresponds to the higher input power in condition B at the lower frequency, which means that more energy was input at each discharge event. Fig. 3 shows the change in the TOC concentration with time under four conditions using oxygen gas. Table 2 shows the reduction rate of the TOC in the treated solution D_{TOC} and the decomposition efficiency of the TOC in the solution η_{TOC} which was calculated based on the experimental data. Since it was difficult to make the initial concentration of acetic acid identical, the value for the vertical axis represents the TOC concentration C normalized by the initial TOC concentration C_0 (30 mgC L^{-1}). Acetic acid was decomposed most sharply under condition A, with 93% of the acetic acid being decomposed after 3 h of treatment. In contrast, while condition B had the same discharge condition as condition A, the decomposition of acetic acid did not proceed even after 3 h and less than 10% of the acetic acid was

decomposed. Under condition C, even though twice the input power of the test under condition A was consumed, the decomposition speed decreased and just 33% of the acetic acid was decomposed. This trend conflicts with the typical trend of the AOP, which exhibits faster decomposition at higher input powers [18]. The treatment under condition D showed a slower decomposition rate than condition C, in the same manner as the comparison between conditions A and B.

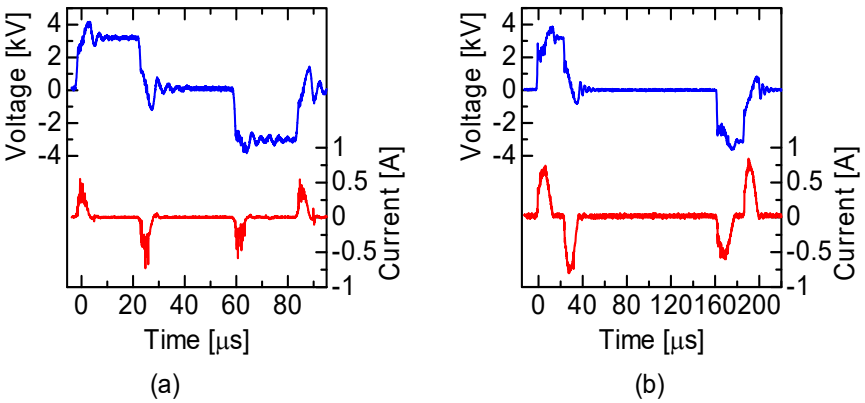

Fig.2. Voltage and current waveforms with O_2 gas supply at (a) 8 kHz with 21 capacitors of 15 pF (condition A and B) and (b) 3 kHz with 21 capacitors of 100 pF (condition C and D).

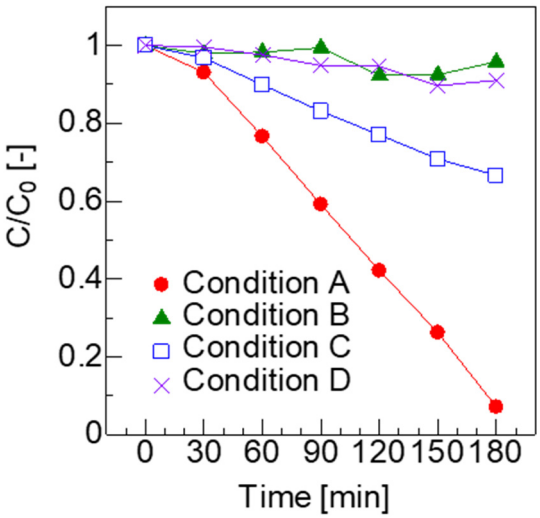

Fig. 3. Change in TOC concentration by plasma in O_2 gas bubbles as a function of treatment time.

Table 2. Decomposition rate and efficiency.

Condition	D_{TOC} [gC h^{-1}]	η_{TOC} [gC kWh^{-1}]
A	7.9×10^{-3} (56% reduction)	0.200 (56% reduction)
B	4.5×10^{-4} (4.2% reduction)	0.011 (4.2% reduction)
C	3.3×10^{-3} (43% reduction)	0.041 (43% reduction)
D	9.0×10^{-4} (9.0% reduction)	0.011 (9.0% reduction)
E	1.7×10^{-3} (16% reduction)	0.061 (16% reduction)
F	8.9×10^{-4} (9.0% reduction)	0.032 (9.0% reduction)
G	2.3×10^{-3} (23% reduction)	0.046 (23% reduction)

As reported previously, when liquid phase hydrogen peroxide and ozone exist at a certain ratio, the reactions represented by eqs. (2)–(6) proceeded [19], and hydroxyl radicals were regenerated from the hydrogen peroxide after the self-quenching reaction as indicated in eq. (7).

$$H_2O_2 + OH^- \rightarrow H_2O + HO_2^- \quad (2)$$

$$O_3 + HO_2^- \rightarrow \cdot OH + O_2 + O_2^- \quad (3)$$

$$O_3 + O_2 \longrightarrow O_2 + O_3^- \quad (4)$$

$$H^+ + O_3 \longrightarrow HO_3\cdot \quad (5)$$

$$HO_3\cdot \rightarrow \cdot OH + O_2 \quad (6)$$

$$H_2O_2 + 2O_3 \rightarrow 2\cdot OH + 3O_2 \quad (7)$$

Under condition A, since hydroxide ions were substantially supplied thanks to the neutral solution, the series of reactions initiated by eq. (2) occurred. The experimental result of the decomposition of acetic acid under condition A shows that the hydroxyl radicals were substantially regenerated by these reactions. In contrast, the result under condition C, under which the decomposition proceeded slowly, compared with condition A, indicates that the regeneration of hydroxyl radicals was suppressed. The results suggest that the higher input energy at each discharge event resulted in a decrease in ozone generation. The higher input energy increases the density of water molecules in the bubbles and the higher density of the water molecules consumes more plasma energy for the generation of hydroxyl radicals rather than for ozone generation, finally generating more hydrogen peroxide [12]. As a result, though there was a plentiful amount of hydroxide ions, as with condition A, condition C did not achieve the reactions shown in eqs. (3) and (4), resulting in a different decomposition rate between conditions A and C.

The results under conditions B and D with low pH achieved a slow decomposition of the acetic acid regardless of the input power, which shows that the pH of the solution greatly affected ozone utilization. The decomposition scarcely progressed even under condition B with an input power of 40 W although the generation of enough ozone was expected considering the results obtained under condition A. This indicated that eq. (2) was not initiated and that hydroxyl radicals were not regenerated under condition B due to the lower pH: corresponding to a lesser concentration of hydroxide ions. Considering the further slower decomposition rate of acetic acid, it is thought that the reason for the slow TOC reduction under condition D was mainly the low pH value, as was the case under condition B.

3.2 Decomposition of acetic acid by plasma in argon bubbles

Fig. 4 shows the representative voltage and current waveforms during plasma generation in argon bubbles. Differing from the cases with oxygen bubbles, double-discharges were caused per cycle due to the selected frequency.

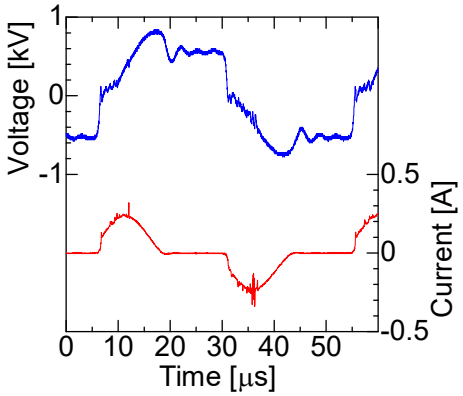

Fig. 4. Voltage and current waveforms with Ar gas supply at 20 kHz with 21 capacitors of 100 pF (condition G).

Fig. 5 shows the change in the TOC concentration with time under conditions E–G. The vertical axis is the TOC concentration with C normalized by the initial concentration C0, in the same manner as Fig. 3. Acetic acid was decomposed by just 16% under condition E and by 9.0% under condition F. Twenty-three percent of the TOC concentration decreased under condition G with twice the input power of conditions E and F, and the decomposition speed was shown to be nearly proportional to the input power. Under these conditions, because of the absence of oxygen molecules, ozone could not be generated, and the regeneration of hydroxyl radicals shown in eq. (7) did not proceed.

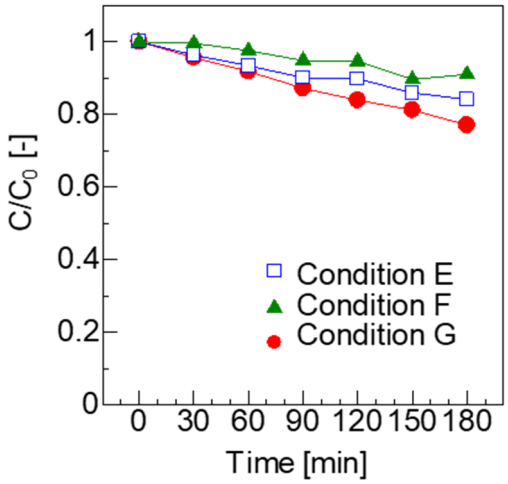

Fig. 5. Change in TOC concentration by plasma in Ar gas bubbles as a function of treatment time.

Unlike the case with oxygen bubbles, the result obtained under the conditions with argon gas indicated that the decomposition speed was determined by the amount of hydroxyl radicals which were directly generated by a reaction of water vapor with electron and metastable Ar (Ar*) with as described in eq. (8), (9): mainly by the reaction described in eq. (8) [18].

$$Ar^* + H_2O \rightarrow Ar + \cdot OH + \cdot H \quad (8)$$

$$e^- + H_2O \rightarrow e^- + \cdot OH + \cdot H \quad (9)$$

The experimental results under conditions E and G show that the pH value of the solution affected the reduction of the TOC in case of processes with argon gas, too. It is assumed that this is because of the difference in the rate constants for the reaction of OH radicals with acetic acids before and after ionization. The rate constants before and after the ionization were 1.6×10^7 L mol^{-1} s^{-1} and 8.5×10^7 L mol^{-1} s^{-1}, respectively [20]. At pH 7.3, most of the acetic acid was ionized while only about 26% of the acetic acid was ionized at pH 4.3. This difference in the ionization rate resulted in a faster reaction between acetic acid and OH radicals at pH 7.3 due to the different rate constant. However, it should be noted that this is not the main reason for the characteristics in cases of plasma in oxygen bubbles since the effect of the pH value of the solution was much smaller in cases with argon gas.

By comparing the results under conditions B and D, the decomposition speed under conditions E and F were almost the same as those under conditions B and D. However, the values in Table 2 show that the decomposition efficiency in cases with argon gas (conditions E and F) was about twice that of cases with oxygen gas (conditions B and D). From this, we confirmed that, as far as the regeneration of hydroxyl radicals did not occur, the total efficiency of generation of hydroxyl radicals was directly determined by the supplied gas and it was higher when argon gas was used rather than oxygen.

3.3 Numerical simulation of TOC reduction

Numerical simulation for the TOC reduction under the four conditions using oxygen gas was implemented using the previously reported model in a commercially available software COMSOL Multiphysics(R) Ver. 5.5 [19]. In this numerical simulation, we calculated generation of hydroxyl radicals and decomposition of organic

compounds in the solution based on generation rates of hydrogen peroxide and ozone shown in Table 3; the generation rate in each condition of input power was measured in a previous study [21]. We assumed that hydrogen peroxide and ozone were supplied at the constant rates and that hydroxyl radicals were generated from them in this simulation. Acetic acid was assumed to be decomposed through the steps shown in eqs. (10) – (14) and the TOC concentration was calculated from the concentration of these acids.

$$\text{Acetic acid} + \cdot\text{OH} \rightarrow \text{Oxalic acid} + CO_2 \quad (10)$$

$$\text{Acetic acid} + \cdot\text{OH} \rightarrow \text{Formic acid} + CO_2 \quad (11)$$

$$\text{Oxalic acid} + \cdot\text{OH} \rightarrow 0.5\text{Oxalic acid} + CO_2 \quad (12)$$

$$\text{Formic acid} + \cdot\text{OH} \rightarrow CO_2 \quad (13)$$

$$\text{Formic acid} + O_3 \rightarrow CO_2 \quad (14)$$

Table 3. Generation rates of hydrogen peroxide G_{H2O2} and ozone G_{O3} applied in the numerical simulation.

Condition	G_{H2O2} [mg h^{-1}]	G_{O3} [mg h^{-1}]
15 pF × 21 (40 W)	14.6	732
100 pF × 21 (80 W)	77.3	144

The ionization of each acid was considered based on their pK_a values and different reaction rates were applied for unionized acids and ionized acids to simulate the reactions [20]. Fig. 6 shows the numerical simulation results of the TOC reduction under two conditions with ballast capacitors of 15 pF and oxygen gas bubbling (conditions A and B). Although the values do not precisely match with experimental results, the trend of the TOC reduction in the numerical simulation coincides with one of the experiments. Fig. 7 shows the numerical simulation result of the TOC reduction under two conditions with ballast capacitors of 100 pF and oxygen gas bubbling (conditions C and D). The trend of this simulation result also coincides with one of the experiments. As discussed regarding the experimental results, the TOC reduction is greatly affected by the solution pH in cases with 15 pF ballast capacitors due to the regeneration process of hydroxyl radicals, while the characteristic scarcely varies with different solution pH in cases with 100 pF ballast capacitors.

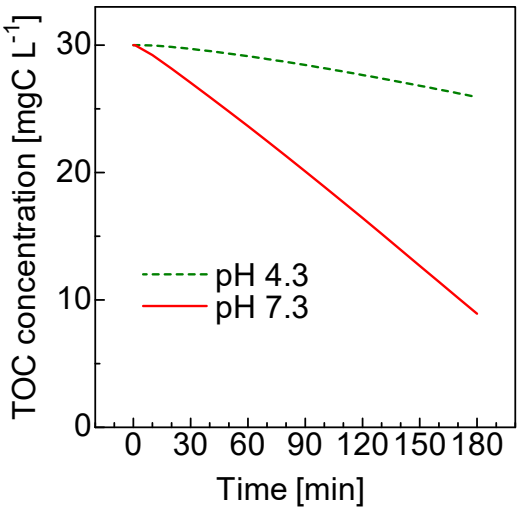

Fig. 6. Simulation result of TOC reduction with ballast capacitors of 15 pF.

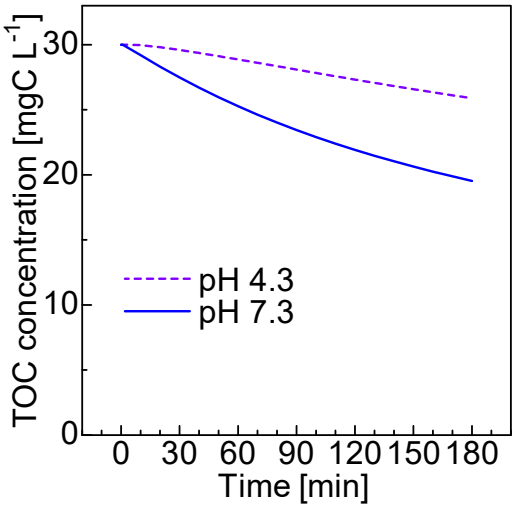

Fig. 7. Simulation result of TOC reduction with ballast capacitors of 100 pF.

4. Conclusion

In this paper, we reported the experimental results of the decomposition of acetic acid using our plasma-based AOP system under various conditions. Detailed analysis on the behavior of ozone was also implemented to scrutinize the reaction mechanism in plasma-based AOP for acetic acid. Acetic acid in a solution of pH 7.3 was decomposed by 93% when 40 W was input to the plasma in oxygen bubbles. However, the decomposition proceeded slowly when the input power was increased due to the reduced generation of ozone. For the solution with a lower pH, an apparent decrease in the decomposition speed was observed due to the absence of the regeneration reactions of hydroxyl radicals. This was at almost the same speed as the case for plasma in argon bubbles, which decomposes acetic acid by hydroxyl radicals directly generated by the plasma. This showed that the decomposition of acetic acid was progressed by hydroxyl radicals originated from the plasma in a low pH solution even when using the plasma in oxygen bubbles, and that the regeneration of hydroxyl radicals caused by ozone could not be utilized.

References

[1] Bostick D. T., Luo H., and Hindmarsh B., Characterization of soluble organics in produced water, Oak Ridge National Laboratory Technical Memorandum ORNL/TM-2001/78 Oak Ridge National Laboratory, TN (https://doi.org/10.2172/814231), 2001.

[2] Strømgren T., Sørstrøm S. E., Schou L, Kaarstad I., Aunaas T., Brakstad O. G., and Johansen Ø., Acute toxic effects of produced water in relation to chemical composition and dispersion, *Marine Environ. Res*., Vol. 40, pp. 147–169, 1995.

[3] Igunnu E. T. and Chen G. Z., Produced water treatment technologies, *Int. J. Low-Carbon Technol*., Vol. 9, pp. 157–177, 2014.

[4] Mizoguchi H. and Takeuchi N., Study of optimal parameters of the H_2O_2/O_3 method for the decomposition of acetic acid, *Chem. Eng. J*., Vol. 313, pp. 309–316, 2017.

[5] Andreozzi R., Caprio V., Insola A., and Marotta R., Advanced oxidation processes (AOP) for water purification and recovery, *Catal. Today*, Vol. 53, pp. 51–59, 1999.

[6] Glaze W. H., Kang J. W., and Chapin D. H., The chemistry of water treatment processes involving ozone, hydrogen peroxide and ultraviolet radiation, *Ozone Sci. Eng*., Vol. 9 (4), pp. 335–52, 1987.

[7] Kosaka K., Yamada H., Shishida K., Echigo S., Minear R. A., Tsuno H., and Matsui S., Evaluation of the treatment performance of a multistage ozone/hydrogen peroxide process by decomposition by-products, *Wat. Res*., Vol. 35 (15), pp. 3587–3594, 2001.

[8] Vittenet J, Aboussaoud W., Mendret J., Pic J.S., Debellefontaine H., Lesage Nicolas, Faucher K., Manero M.H., Thibault-Starzyk F., Leclerc H., Galarneau A., and Brosillon S., Catalytic ozonation with γ-Al_2O_3 to enhance the degradation of refractory organics in water, *Appl. Catal. A: Gen*., Vol. 504, pp. 519–32, 2015.

[9] Matsui Y., Takeuchi N., Sasaki K., Hayashi R., and Yasuoka K., Experimental and theoretical study of acetic acid decomposition by a pulsed dielectric-barrier plasma in a gas-liquid two-phase flow, *Plasma Sources Sci. Technol*., Vol. 20 (3), pp.034015, 2011.
[10] Saeki R., Tachibana K., Kamiya Y., Mizoguchi H., Takeuchi N., and Yasuoka K., Mineralization of highly conductive and contaminated produced water using an oxidation system combining diaphragm discharge and ozone, *J. Inst. Electrostat. Jpn*., Vol. 40 (2), pp. 90–95, 2016. (in Japanese)
[11] Ishiguro T. and Yasuoka K., Advanced oxidation process by a combined ozone/plasma system using plasma in bubbles, *IEEJ Trans. FM*, Vol. 135 (3), pp. 175–181, 2015. (in Japanese)
[12] Takeuchi N., Ishii Y., and Yasuoka K., Modelling chemical reactions in DC plasma inside oxygen bubbles in water, *Plasma Sources Sci. Technol*., Vol. 21 (15), pp. 015006, 2012.
[12] Lukes P., Appleton A. T., and Locke B. R., Hydrogen peroxide and ozone formation in hybrid gas-liquid electrical discharge reactors, *IEEE Trans. Plasma Sci*., Vol. 40 (1), pp. 60–67, 2004.
[13] Magureanu, M., Piroi, D., Gherendi, F., Mandache, N.B., and Parvulescu, V., Decomposition of methylene blue in water by corona discharges, *Plasma Chem. Plasma Proc*., Vol. 28 (6), pp. 677–688, 2007.
[14] Bradu, C., Magureanu, M., and Parvulescu, V.I., Degradation of the chlorophenoxyacetic herbicide 2,4-D by plasma-ozonation system, *J. Haz. Mat*. Vol. 336, pp. 52–56, 2017.
[15] Magureanu, M., Mandache, N.B., Bradu, C., and Parvulescu, V.I., High efficiency plasma treatment of water contaminated with organic compounds. Study of the degradation of ibuprofen, *Plasma Processes Polym*., Vol. 15 (6), pp.1700201, 2018.
[16] Shimizu T., Iwafuchi Y., Morfill G. E., and Sato T., Transport mechanism of chemical species in a pin-water atmospheric discharge driven by negative voltage, *J. Photopolym. Sci. Technol*., Vol. 24 (4), pp. 421–427, 2011.
[17] Kuroki T., Yoshida K., Watanabe H., Okubo M., and Yamamoto T., Decomposition of trace phenol in solution using gas-liquid interface discharge, *Jpn. J. Appl. Phys*., Vol. 45 (5A), pp. 4296–4300, 2006.
[18] Takeuchi N., Ando M., and Yasuoka K., Investigation of the loss mechanisms of hydroxyl radicals in the decomposition of organic compounds using plasma generated over water, *Jpn. J. Appl. Phys*., Vol. 54 (11), pp. 116201, 2015.
[19] Takeuchi N. and Mizoguchi H., Study of optimal parameters of the H_2O_2/O_3 method for the decomposition of acetic acid, *Chem. Eng. J*. Vol. 313, pp. 309–316, 2017.
[20] Karpel Vel Leitner N. and Dore M., Hydroxyl radical induced decomposition of aliphatic acids in oxygenated and deoxygenated aqueous solutions, *J. Photochem. Photobiology A: Chem*., Vol. 99 (2–3), pp. 137–143, 1996.
[21] Takeuchi, N., Ishibashi, N., Sugiyama, T., and Kim, H.H., Effective utilization of ozone in plasma-based advanced oxidation process, *Plasma Sources Sci. Technol*., Vol. 27 (5), pp. 055013, 2018.